



PARAMETER SENSITIVITY OF 12S-10P HEFSM WITH IRON FLUX BRIDGES FOR HEV APPLICATIONS

Nurul 'Ain Jafar, Erwan Sulaiman and Siti Khalidah Rahimi

Research Center for Applied Electromagnetics, Universiti Tun Hussein Onn Malaysia, Parit Raja, Batu Pahat, Johor, Malaysia

E-Mail: aienjafar@yahoo.com

ABSTRACT

The demand of conventional vehicles which operates with internal combustion engine (ICE) has been increased with the increasing of the world population. However, it has led to the pollutant emissions which would affects to the global warming. Thus, to overcome this problem, auto-manufacturers has been introduced hybrid electric vehicles (HEVs) which combined the ICE with battery based electric motor. Many researchers has been focus on a new machine which are known as flux switching machine. HEFSM becomes as a one possible candidates among the other FSMs due to the flux sources. Thus, a new structure of 12S-10P HEFSM with additional iron flux bridges has been developed to overcome the problem of C-Type stator core. Therefore, some design optimization is conducted to achieve the target torque and power which similar to the requirement of conventional HEVs, Prius '07. As a result, the optimum design has been successfully achieve the target torque and power, respectively.

Keywords: iron flux bridges, permanent magnet, hybrid excitation.

INTRODUCTION

The conventional vehicles operate on the principle of internal combustion engine (ICE) which based on fossil fuels have been used in over than hundred years for personal transportation. The growing demand for ICE based vehicles for personal mobility has led to significant increase in crude oil consumption and concern on energy security. With ever increasing use of ICE for personal mobility, the CO₂ and pollutant emissions pose a serious concern on global warming and environment (Chan, 2007). Hence, ICE automobile becomes a major source of the urban pollutions due to the high demand and usage of personal vehicles. Besides air pollution, the other main objection regarding ICE automobiles is its extremely low efficiency use of fossil fuel (Kim *et al.* 1999). A potential solution to reduce the harmful pollutant emissions and prevent global warming in vehicles is by employing electric motors as propulsion drives.

Thus, in order to tackle these major issues, auto-manufacturers are shifting towards new technologies such as hybrid electric vehicles (HEVs). HEV technologies are extensively attracted to researchers in recent years for the environmental consciousness of related fields and also offer the most promising solutions to reduce the emission (Lin and Chan, 2012). The HEV has an uniqueness of the energy which can be fed back into the battery for storage, e.g., during regenerative braking (which is otherwise wasted as heat in a conventional vehicle). Nowadays, Toyota and Honda which well-known car manufactures has been established HEV cars i.e Prius and Insight, respectively. Among the consumers, both of these cars are getting more popular due to their incredible mileage and less emissions. Besides that, the other auto-manufacturers also marketing their HEVs for general populations likes

Mitsubishi, Renault, DaimlerChrysler, Fiat, GM, Nissan, Subaru and Ford (Butler *et al.* 1999). Although the number for alternative electric vehicles is not significantly higher when efficiency is evaluated on the basis of conversion from crude oil to traction effort at the wheels, it makes a difference.

As one of the successful electric machines, Interior Permanent Magnet Synchronous Motors (IPMSM) has been selected by auto-manufacturers which commercialized in HEVs. It is because this electric machine can be utilized as a main traction motor in terms of high efficiency over most of operating torque-speed range and high torque and/or power density. Apart from that, it should take consideration about the restriction of motor size to ensure the enough space for passenger and also the limitation of motor weight to reduce fuel consumption (Ozawa *et al.* 2009). However, these machines have disadvantages of distributed armature windings which caused longer coil end length and gives high copper losses. In addition, the rotor geometry and construction in IPMSM is less robust due to the PM is located on the rotor part thus unsuitable in high speed applications (Sulaiman *et al.* 2010). Another problem is the shape in IPMSM is difficult to shape and optimize. Besides, this machine needed high PM volume which lead to high manufacturing cost (Sulaiman *et al.* 2011). Due to this problem, a better machine such as flux switching machine (FSM) is selected which has rugged rotor structure suitable for high-speed operation while keeping high torque and power density.

Among FSMs candidates, hybrid excitation flux switching machine (HEFSM) has been chosen (Hoang *et al.* 2007), (Emmanuel *et al.* 2009) and well-suitable choice for HEVs respects to their flux sources with the additional



field excitation coils (FECs). HEFSM becomes more attractive because it combines both flux sources from PMs and FECs, respectively. Over the years, HEFSM becomes getting interest from researchers due to advantages of easy cooling and robust rotor structure which suitable for high speed applications (Owen *et al.* 2010), (Kosaka *et al.* 2010). In the machine configuration, all active parts such as armature coils, PMs and FECs are employed in the stator part. This machine not only a simple rotor body with mechanically rugged structure but similar with the switched reluctance machine which is ease of cooling all active parts. Figure-1 illustrates the topology of 12S-10P C-Type HEFSM with additional of iron flux bridges. The additional of iron flux bridges to the machine design can overcome the problem of separated stator core which lead to difficulty in manufacturing design as well as flux leakage to the outer stator. In addition, the main objectives of adding the iron flux bridges to the initial design motor not only can solve the manufacture process but also can enhance the effectiveness of the FEC with various excitation flux level. Through the cross sectional depicts in Figure-1, the stator is consists of 12 segments of C-Type cores with both of 12 PMs and FECs are aligned together which attached in between the armature coils. In addition, the width of iron flux bridges is set to 0.5mm.

WORKING PRINCIPLE OF HEFSM

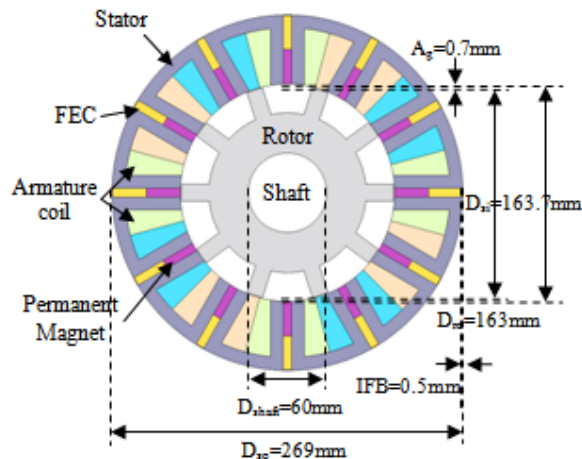


Figure-1. Initial design of 12S-10P C-Type HEFSM with iron flux bridges.

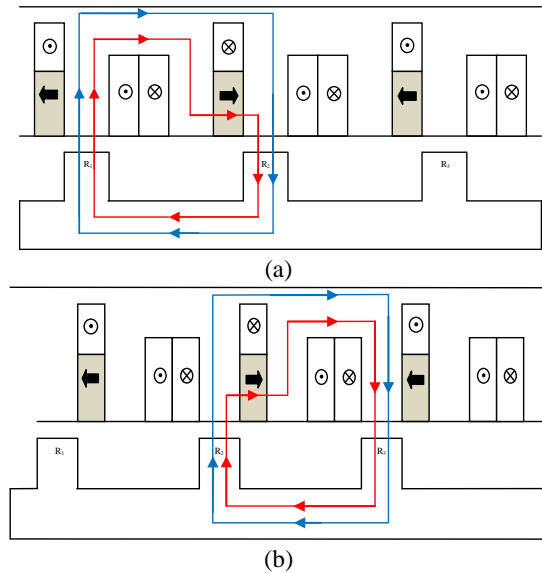


Figure-2. The operating principle of HEFSM
(a) R1 bringing flux (b) R2 bringing flux.

The working principle of the presented HEFSM is demonstrated in Figure-2. From the figure, the red and blue line signified the PM flux and FEC flux, correspondingly. As illustrates in Figure-2(a), while the direction of both PM and FEC fluxes are in the same polarity, both fluxes are combined and shift together from stator to the rotor pole R_2 and return back to the stator through rotor pole R_1 . At this condition, rotor pole R_1 brings flux to the rotor while rotor pole R_2 receives flux from stator hence producing more fluxes with a so called hybrid excitation flux. In addition, when the rotor moves to the left side approximately half electric cycles, as shown in Figure-2(b), it illustrates rotor pole R_3 receiving flux from stator while R_2 bring flux. Furthermore, the changes of flux of R_2 to R_3 have been proved that the flux has been switched of original polarity to another polarity thus the concept of flux changes is called as FSM.

DESIGN RESTRICTIONS AND SPECIFICATIONS

Table-1 lists the design restrictions and target specifications of the proposed machine which similar to the conventional HEVs. The maximum DC-bus voltage inverter and inverter current which related to the electric restrictions are set to 650V and 360A_{rms}, correspondingly. In addition, the limitation of the armature current density and field excitation current density are set to the maximum of 30A_{rms}/mm² and 30A/mm², respectively by assume only a water cooling system is employed as a cooling system for the machine. Other than that, the PM weight is set to the 1.3kg which NEOMAX35AH is used as a PM material. Other than that, the materials are used for stator and rotor body is electric steel 35H210 whereas cooper are used for armature coils and FECs. For the machine



performances, the target requirement for torque and power are set 303Nm and 123kW, correspondingly. Commercial FEA package, JMAG-Studio ver.10.0, released by Japanese Research Institute (JRI) is used as 2D-FEA solver for this design.

DESIGN OPTIMIZATION PROCEDURE

The initial performances in terms of torque and power for the proposed machine as shown in Figure-1 are obtained. Design optimization is conducted in order to achieve the maximum target in term of torque and power performance. The maximum torque and maximum power obtained are 189.6Nm and 20.7kW, respectively, which is

Table-1. Design restrictions and target specifications of the proposed HEFSM.

Descriptions	HEFSM
Max. DC-bus voltage inverter (V)	650
Max. inverter current (A_{rms})	360
Max. current density in armature coil, J_a (A_{rms}/mm^2)	30
Max. current density in FEC, J_e (A/mm^2)	30
Stator outer diameter (mm)	269
Motor stack length (mm)	84
Air gap length (mm)	0.7
PM weight (kg)	1.3
Maximum torque (Nm)	303
Maximum power (kW)	123
Iron flux bridge width (mm)	0.5

far from the target requirement. In order to increase the target torque and power, design free parameters A_1 until A_9 are identified in rotor and stator part as described in **Figure-3**. Basically, the design parameters are divided into four groups such as related to rotor part, permanent magnet slot shape, field excitation slot shape and armature slot shape. In the figure, the rotor parameters are marked as A_1 , A_2 and A_3 , the permanent magnet are marked as A_4 and A_5 , the field excitation slot shape parameters are A_6 and A_7 , and armature slot shape parameters are A_8 and A_9 , respectively.

The first step is bring out by updating rotor parameters, A_1 , A_2 and A_3 while keeping A_4 to A_9 constant. As the torque increases with the increasing of rotor radius, A_1 is considered as the dominant parameter to improve the torque. **Figure-4**, **Figure-5** and **Figure-6** demonstrates the torque and power performances of A_1 , A_2 and A_3 , correspondingly. From the **Figure-4**, the torque is maximum when the rotor radius is set to 83.5mm. In

addition, both of the rotor pole height, A_2 and the rotor pole width, A_3 are varied by kept A_1 at 83.5mm until the combination of maximum torque and power are achieved. The maximum torque and power that obtain are 203.6Nm and 24.0kW when A_2 is 23.1mm and A_3 is 8.3mm, respectively. From the result, it noticed that torque and power increased with longer rotor radius, longer rotor height and larger pole width. In addition, it is due to the rotor have enough space to get the flux flow from stator. Furthermore, the next step of the design is carried

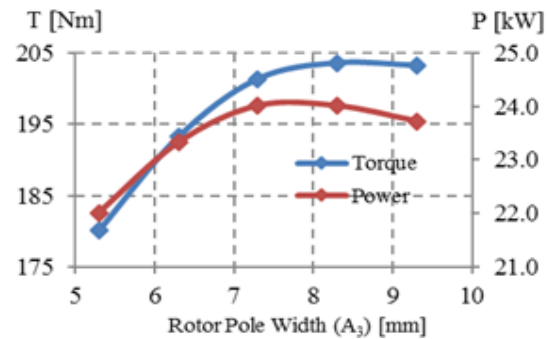


Figure-6. Torque and power versus rotor pole width,

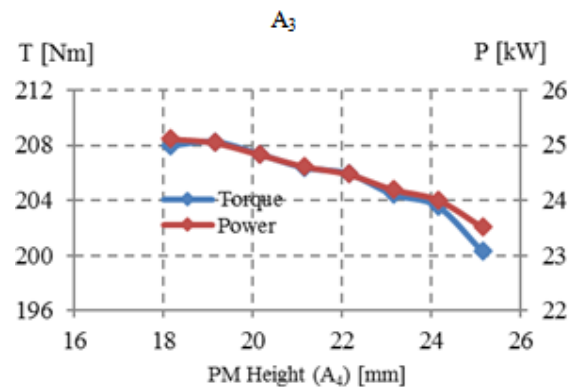


Figure-7. Torque and power versus PM height, A_4 whereas for A_5 , A_6 various to A_4 .

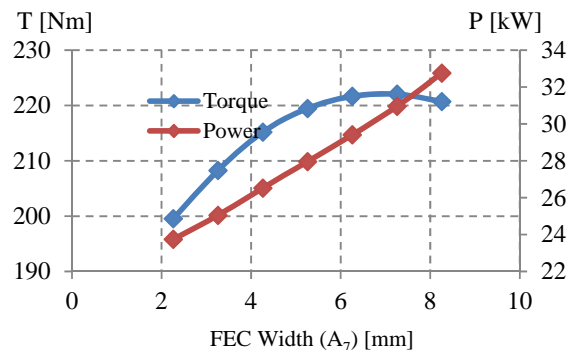


Figure-8. Torque and power versus FEC width, A_7 .



torque is increased by reduction of stator back iron width, A_8 and stator teeth width, A_9 which can reduced the S_a and also number of armature coil turn, N_a as illustrated in Figure-9 and Figure-10, correspondingly. At this step, the torque and power performance is increased up to 282.6Nm and

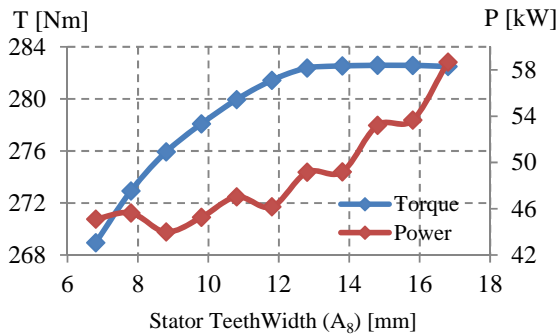


Figure-9. Torque and power versus stator teeth width, A_8 .

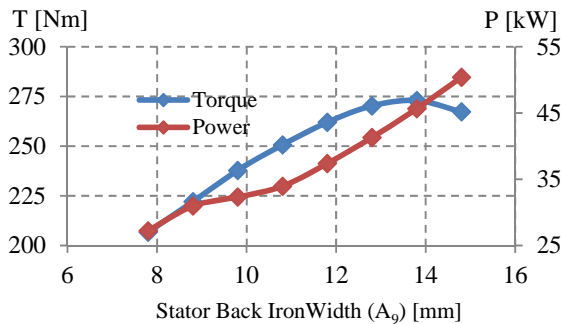


Figure-10. Torque and power versus stator back iron width, A_8 .

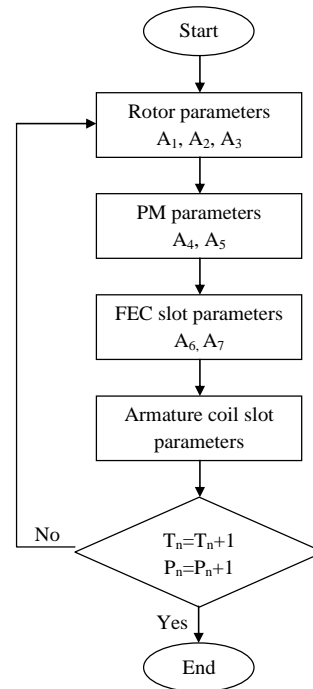


Figure-11. Deterministic optimization method.

53.2kW, respectively.

This design process is repeated by adjusting A_1 to A_9 until the optimum torque and power are achieved. Figure-11 depicts the method of optimization or also known as deterministic optimization method. Finally, the optimum torque and power of 312.5Nm and 134.2kW with 1.3kg of PM after 5 cycle of optimization is conducted are listed in Figure-12. Besides that, the final design of this machine which satisfies the target performance is illustrated in Figure-13.

DESIGN RESULTS AND PERFORMANCE PREDICTIONS OF INITIAL AND OPTIMUM DESIGN

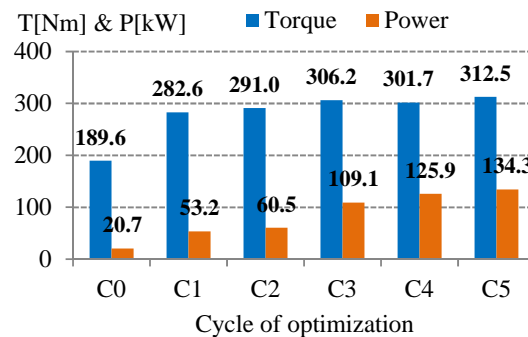


Figure-12. Torque and power versus cycle of optimization for 12S-10P HEFSM.

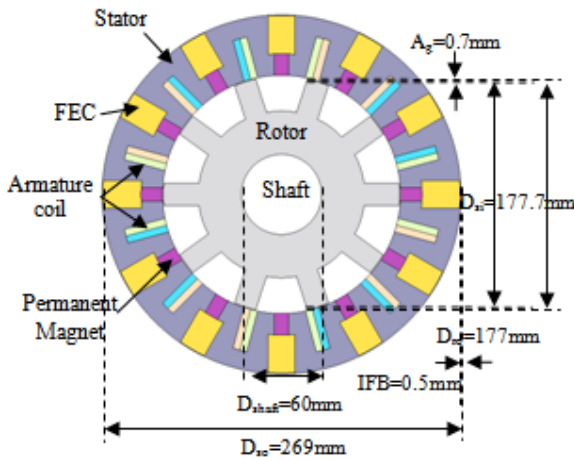


Figure-13. Final design of 12S-10P HEFSM.

Flux distribution under no load condition

The comparison of flux distribution for the initial and optimum 12S-10P HEFSM under PM with maximum J_e of $30\text{A}/\text{mm}^2$ are presented in Figure-14. From the graph, it is obvious that the stator teeth width of the optimum design is expanded to give more flux flows easily. In addition, the flux leakage to the outer stator at the initial design has been reduced.

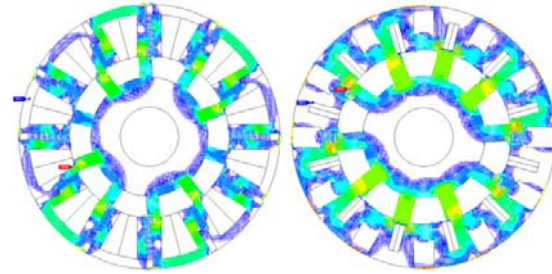


Figure-14. Flux distribution under no load condition.

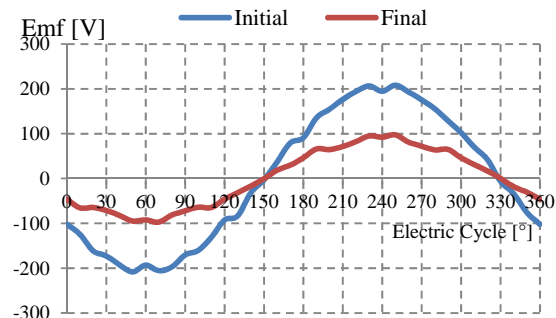


Figure-15. Back-emf at rated speed 1200 r/min.

Back-emf under no load condition

The back-emf for the initial and optimum design of the proposed machine that generated at rated speed of 1200r/min is illustrated in Figure-15. At this condition, the voltage with J_e of 0A means that the induced voltage is produced from PM flux only. From the graph, it clearly shows that the optimum design has more sinusoidal back-emf compared with the initial design. Moreover, the amplitude of fundamental component for final design has been reduced from 208.1V to 97.5V, which is approximately 53.1% of amplitude reduction.

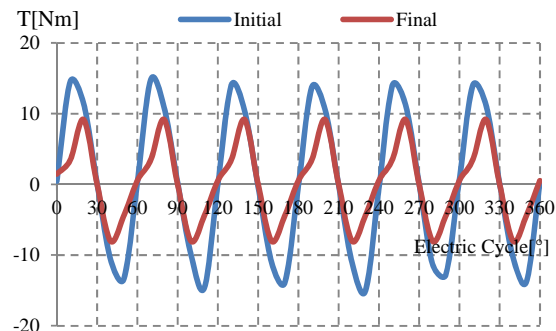


Figure-16. Cogging torque under the conditions of PM with maximum FEC current density of $30\text{A}/\text{mm}^2$.

Cogging torque under no load condition

Figure-16 shows the cogging torque of the optimum design compared to the initial design under the conditions of PM with maximum FEC current density of $30\text{A}/\text{mm}^2$. Obviously, 6 cycles of cogging torque are generated to complete one electric cycle. Based on the graph, it obviously shows that the peak-peak of final design has reduced which approximately 43% of initial design from 30.0Nm to 17.2Nm.

Torque versus field excitation current density, J_e at various armature current densities, J_a under load condition

The torque versus field excitation current density,

J_e at various armature current densities, J_a for final design is plotted in Figure-17. Through the graph, the torque is increased with the increasing of J_e and J_a up to the certain value. While the maximum torque is achieved when J_e and J_a are set to $30\text{A}/\text{mm}^2$ and $30\text{A}_{\text{rms}}/\text{mm}^2$, correspondingly of approximately 312.5Nm with the increment about 39.3% than initial design and achieved the target specifications for the HEV applications.

Torque and power versus speed characteristics

The torque and power versus speed characteristics of the initial and optimum design HEFSM is demonstrated in Figure-18. From the graph, the blue and red lines indicate the initial maximum torque and power curve, correspondingly. While the orange and purple lines



depict the torque and power of the optimum design. Obviously, the maximum torque obtained is 312.6Nm at the base speed 4102 r/min with corresponding power of 134.2kW. The final design has increased 39.2% and 84.6% in torque and power, respectively.

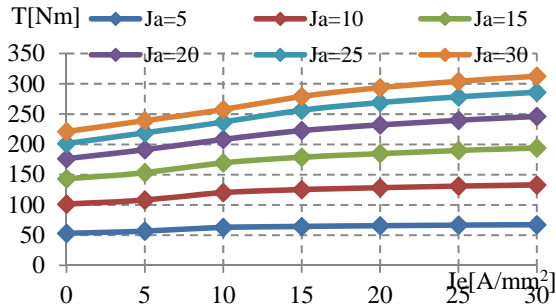


Figure-17. Torque versus J_c at various J_a for final HEFSM.

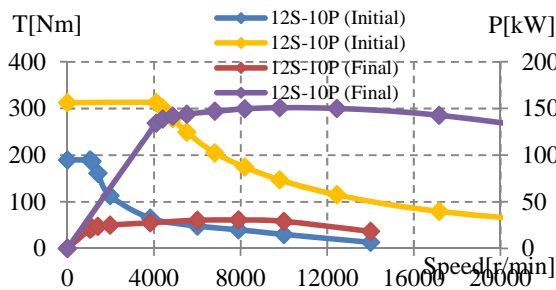


Figure-18. Torque and power vs speed curve for initial and final of 12S-10P HEFSM.

Motor loss and efficiency

The motor loss and efficiency are calculated by finite element analysis considering copper losses in the armature winding and iron losses in all laminated cores. The specific operating points at the maximum torque, maximum power and frequent operating point under light load driving condition for 12S-10P HEFSM noted as No.1 to No.8 is presented in Figure-19. Meanwhile, the detailed loss analysis and motor efficiency of the designed machine are summarized in Figure-20. In the graph, P_o is the total output power, P_i is the iron loss and P_c is the total copper loss. It can be expected that the designed machine realizes good efficiency at the maximum torque (No.1) and the maximum power (No.2). At high torque operating points No.1, the motor efficiency is 83.2% although it has high copper loss. In addition, at high power operating points No.2, the efficiency is 77.7% and slightly degraded due to the increase in copper loss. Furthermore, at frequent driving operation No.3 to No.8 under low load condition, the proposed machine achieves relatively high-efficiency more than 85%.

Magnet demagnetization analysis at high temperature

The maximum temperature for motor drive in HEVs is assumed to reach around 180°C. The temperature condition is set to 180°C for evaluation of demagnetization as the worst case. The demagnetization factor of permanent magnet (NEOMAX35AH) used in this machine is calculated from,

$$\%D = \frac{\text{volume of PM demagnetized}}{\text{total volume of PM}} \quad (1)$$

To identify whether an element of permanent magnet is demagnetized or not, the knee point on the demagnetization curve is referred. The calculated results show that permanent magnet demagnetization that used in

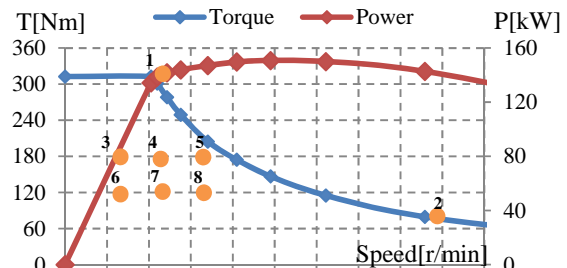


Figure-19. Frequent operating point of HEV for 12S-10P HEFSM.

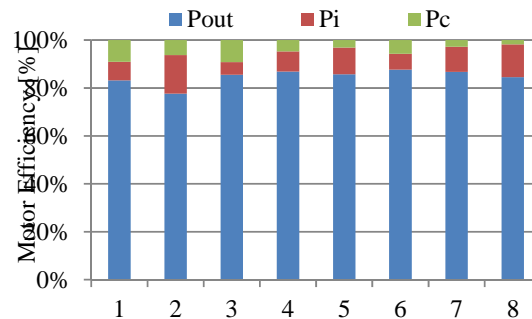


Figure-20. Motor loss and efficiency for 12S-10P HEFSM.



Figure-21. Flux vector density.

the design of 12S-10P HEFSM has 0.21% when operating in high thermal condition as shown in flux vector density in Figure-21.

CONCLUSIONS

In this paper, a new structure of 12S-10P HEFSM with iron flux bridges has been discussed. The design optimization procedure to bring out the optimum torque and power has been explained. In addition, the performances of the final design is satisfied with the design constraint and requirement which similar to the conventional HEVs. Thus, the optimum torque and power of this machine has increased up to 39.2% and 84.6%, respectively compared with the initial design.

ACKNOWLEDGEMENT

This work was supported by Research Innovation, Commercialization and Consultancy Management (ORICC) with Vot No E15501, FRGS 1508 and ERGS 030, Universiti Tun Hussein Onn Malaysia (UTHM), Batu Pahat, Johor and Ministry of Education Malaysia (MOE).

REFERENCES

- Butler, K.L., Ehsani, M. and Kamath, P. 1999. A Matlab-based modeling and simulation package for electric and hybrid electric vehicle design. *IEEE Transactions on Vehicular Technology*, 48(6), pp.1770-1778.
- Chan, C.C. 2007. The state of the art of electric, hybrid, and fuel cell vehicles. *Proceedings of the IEEE*, 95(4), pp. 704–718.
- Emmanuel, H. et al., 2009. Experimental Comparison of Lamination Material Machine presentation Experimental test bench presentation Measurement presentation. *Currents*, 2(33), pp. 1–7.
- Hoang, E., Lecrivain, M. and Gabsi, M. 2007. A new structure of a switching flux synchronous polyphased machine with hybrid excitation. 2007 European Conference on Power Electronics and Applications, EPE.
- Kim, P.-S.K.P.-S., Kim, Y.K.Y. and Hong, B.-Y.H.B.-Y. 1999. A method for future cost estimation of hybrid electric vehicle. *Proceedings of the IEEE 1999 International Conference on Power Electronics and Drive Systems. PEDS'99 (Cat. No.99TH8475)*, 1(July), pp.315–320.
- Kosaka, T. et al. 2010. Design studies on hybrid excitation motor for main spindle drive in machine tools. *IEEE Transactions on Industrial Electronics*, 57(11), pp.3807–3813.
- Lin, C.-P. and Chan, I.-H. 2012. Fuzzy Nonlinear Programming Based Life Cycle Cost Optimization for Hybrid Electric Vehicles. 2012 International Symposium on Computer, Consumer and Control, pp. 282-285.
- Owen, R.L., Zhu, Z.Q. and Jewell, G.W. 2010. Hybrid-excited flux-switching permanent-magnet machines with iron flux bridges. *IEEE Transactions on Magnetics*, 46(6), pp. 1726-1729.
- Ozawa, I., Kosaka, T. and Matsui, N. 2009. Less rare-earth magnet-high power density hybrid excitation motor designed for Hybrid Electric Vehicle drives. 2009 13th European Conference on Power Electronics and Applications, (1).
- Sulaiman, E., Kosaka, T. and Matsui, N. 2011. Design Optimization of 12Slot - 10Pole Hybrid Excitation Flux Switching Synchronous Machine with 0.4kg Permanent Magnet for Hybrid Electric Vehicles.
- Sulaiman, E., Kosaka, T. and Matsui, N. 2010. FEA-based design and parameter optimization study of 6-slot 5-pole PMFSM with field excitation for hybrid electric vehicle. *PECon2010 - 2010 IEEE International Conference on Power and Energy*, pp. 206-211.